PHYSICAL REVIEW A VOLUME 25, NUMBER 2 FEBRUARY 1982

Auger spectra excited in collisions of fast phosphorus ions with thin carbon foils

D. Ridder* and D. Schneider
Hahn-Meitner-Institut für Kernforschung Berlin GmbH, Bereich Kern- und Strahlenphysik, Glienicker Strasse 100, 1000 Berlin 39, West Germany
(Received 5 May 1981)

Auger-electron spectra have been measured following excitation of 100-500-keV phosphorus ions by thin carbon foils. The spectra are rich in structure mostly due to Auger-satellite transitions. The composition of the Auger spectrum is interpreted with the aid of nonrelativistic Hartree-Fock calculations. In the low-energy portion, several lines could be identified. Based on calculated energies for groups of Auger transitions, the high-energy part can also be interpreted. We observe a general increase of the high-energy feature—distinct peaks as well as the gross structure—with decreasing projectile velocity. Two processes may be responsible for this variation: the enhanced production of double L vacancies and the increased capture of target electrons into excited levels of the projectile ions.

I. INTRODUCTION

Recently, the Auger yield of phosphorus ions following foil excitation has been found to be unexpectedly high.[1] These findings gave some hope to use phosphorus or similar elements as an active medium for the development of an x-ray laser.[2] For a complete understanding of the mechanism responsible for the high vacancy production rate, it is necessary to study this collision system in more detail. Hence, we try to give spectroscopic assignments of lines and examine the intensities yielding information on the excitation process and the decay probabilities.

Early studies of Auger-electron spectra were concerned with rare gases.[3] In those cases relatively simple spectra were observed following excitation by fast electrons. Light projectiles produce mainly singly ionized target ions and the resulting configurations for the initial states of the Auger decays are simple in the sense that they consist mostly of only up to two incomplete shells with few vacancies. The angular-momentum coupling of the electrons in these shells leads to only few initial terms and correspondingly only few allowed transitions are observed.

Only several years ago, the more complicated spectra of elements with incomplete outer shells have been studied.[4] The number of possible Auger transitions for these elements is very large because the angular-momentum coupling for the electrons in the depleted shells leads to a multitude of terms. A maximum of possible terms is achieved for elements with half-filled outer shells such as phosphorus. However, when using foil excitation, we hope to eject many of these outer-shell electrons in parallel to the production of a vacancy in an inner shell. This should lead again to relatively simple spectra due to the above arguments concerning the number of possible terms. On the other hand, the foil-excitation mechanism is a very complex process and introduces new disturbances by multiple ionization of the inner-shell and additional excitation of outer-shell electrons. Also charge-exchange processes are expected to play an important role.

The first measurements of phosphorus Auger-electron spectra were reported in connection with energy-loss studies in the collision system P^+-Ar.[5] In those measurements, multiple L-shell excitation of various lower-Z projectiles impinging on argon was observed. A spectroscopic examination of phosphorus Auger data was presented five years later.[6] In that work also, spectra of neighboring elements were presented and examined in parallel. Several features, especially in the low-energy portions of the spectra were identified using semiempirical energies. It was observed that the lines in the low-energy structure are due to second transitions in an Auger cascade following double-vacancy production in an inner shell.

Phosphorus target spectra have been measured in the collision systems 60-keV Ar^+ on GaP and InP.[7] However, due to binding- and solid-state effects the diagram lines were shifted and the resolu-

tion was poor. In comparison with our calculations the observed transitions $L_{23}M_1^2$ and $L_{23}M_1M_{23}$ were too low by about 19 and 16 eV, respectively. This is beyond the error of our Hartree-Fock results and reflects the influence of neighboring atoms on the outer-shell electrons.

As a large part of this work is concerned with a presentation of calculated transition energies for Auger decays of very different types, we review in Sec. II a classification and present the appropriate spectroscopic notations. The third part will then be dedicated to the spectroscopic analysis. In Sec. IV we analyze the intensity variation of the spectra at impact energies of 100–500 keV. In Sec. V, conclusions are drawn and an outline for future developments is given. The experimental setup and method were presented in an earlier paper.[8] In the present work very small observation angles ($\sim 9°$) were used in order to minimize kinematic line broadening.

II. TYPES OF AUGER TRANSITIONS

A comprehensive classification of Auger decays has been given some years ago.[9] Mainly six types ($A-F$) of Auger transitions are distinguished. Type A involves all normal Auger transitions following the production of a single inner-shell vacancy. A typical normal Auger decay of a $2p$ vacancy will be described either in the form $L_{23}-M_{23}^2$ or $2p^5-3s^23p$ (in the case of phosphorus). Starting with type B, the following transitions are called satellites: B satellites arise from inner-shell excitation, where for subgroup B_α the excited electron is not involved in the decay and for B_β it is involved. The relevant notations are, e.g., $2p^53s^23p^34s - 2p^63s^23p4s$ for B_α lines and $2p^53s^23p^34s - 2p^63s^23p^2$ for B_β lines. The initial state for C satellites is produced by ionization of the inner-shell electron and monopole excitation (i.e., excitation to the same angular-momentum quantum number) of an electron from an outer shell. Lines of type D evolve from initial states with two vacancies, one inner-shell and one outer-shell vacancy. This type of transition is the most common type of satellites following ionization by light particles, and is described as either $L_{23}M_1 - M_1^2M_{23}$ or $2p^53s\,3p^3 - 2p^63s^03p^2$. Satellites with many outer-shell vacancies which play an important role in our spectra fall beyond the classifications of Ref. 9 and are summarized as type-X transitions. For completeness, types E and F are rarely observed and correspond to initial states with more than two excited electrons and double Auger transitions, respectively.

III. SPECTROSCOPIC ANALYSIS

In this part we analyze the phosphorus Auger structure on the basis of calculated transition energies using a nonrelativistic Hartree-Fock program.[10] The term energies were calculated using the proper coefficients for Slater integrals obtained by means of an angular-momentum coupling program.[11] The spin-orbit splitting was calculated for a typical case (Fig. 2) using a standard computer code,[12] and was found to be of minor importance here.

In the beginning, we give a rough overview over the shape of the spectrum and dominating line groups. Figure 1 shows a typical Auger spectrum of the phosphorus projectile following passage through a carbon foil of 10 μg/cm^2 thickness. The spectrum was measured at an impact energy of 500 keV and was corrected for the Doppler shift. Hence, the energy scale refers to the projectile's rest frame. The linewidths observed in this spectrum still reflect the influence of kinematical effects. Natural linewidths may be smaller by approximately one order of magnitude. The spectrum displayed here was obtained after subtraction of a background intensity of electrons with continuous energy distribution. The subtraction was performed using a second-order polynomial fit to the background on both sides of the Auger structure to represent the continuous energy distribution.[13]

Calculated average transition energies for Auger decays of the type $L_{23}^kM^i-L_{23}^{k-1}M^{i+2}$ ($k=1,2,3$ and $i=0,1,2,3$) are indicated above the spectrum. Figure 1 shows that the low-energy portion of the spectrum should be due to satellite transitions of the kind $L_{23}M^3-M^5$ with a high degree of outer-shell ionization. For the high-energy part, we have to assume transitions due to low outer-, but high inner-shell ionization as for example $L_{23}^2-L_{23}M^2$. Still higher degrees of inner-shell ionization should be less probable. However, the spectrum extends to rather high energies. If in the initial state of an Auger transition one of the outer electrons is raised by shake-up to some higher orbital, e.g., from $3s$ to $5s$, or an electron is captured into a high orbital following the inner-shell ionization, the transition energy of the decay with the excited electron being involved in the decay (groups B_β, C_β, etc.) is higher than the energy of the decay of the state

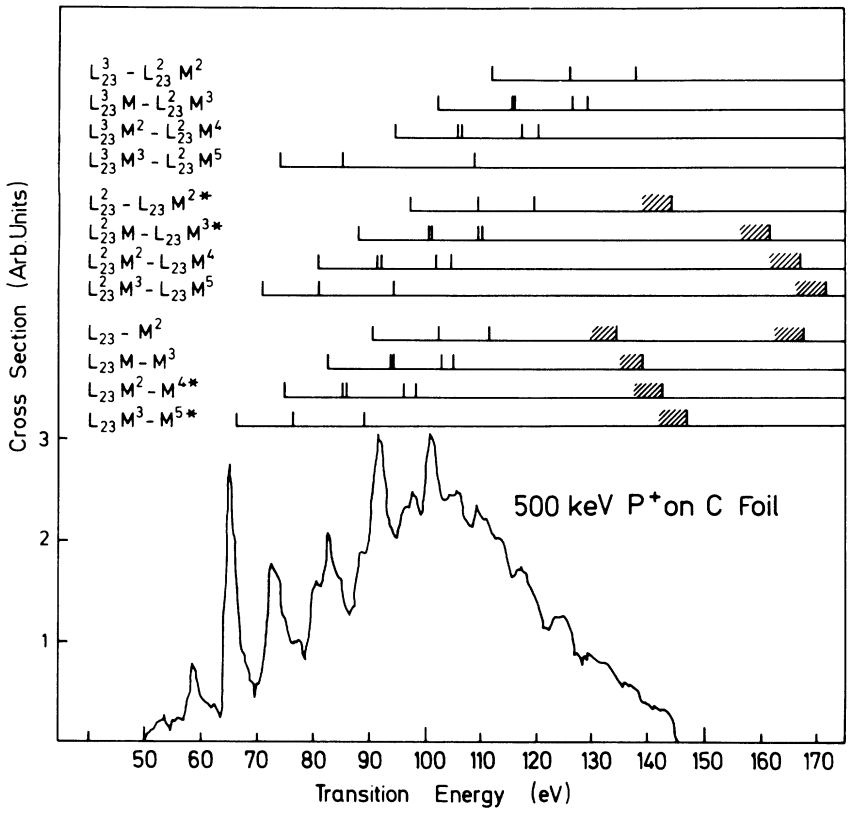

FIG. 1. Typical Auger spectrum of phosphorus projectiles at 500-keV impact energy after foil excitation. A continuous background has been subtracted and the kinematic energy shift was eliminated. Calculated average transition energies for normal Auger transitions $L_{23}-M^2$ and satellite transitions $L_{23}^k M^i - L_{23}^{k-1} M^{i+2}$ ($k=1-3$, $i=0-3$) are indicated. The upper limit for transitions with one electron excited to a higher level is shown.

with the electron in its usual orbital. All these transition energies have an upper limit where the orbital quantum number of the excited electron approaches infinity, e.g., $2p^3 3s\,3p^2 nl \rightarrow 2p^4 3s\,3p$ ($nl \rightarrow \infty$), indicated as series limits in Fig. 1. A second limit results from similar transitions with two electrons being excited to higher orbitals and taking part in the Auger decay, e.g., $2p^3 3p^2 nl^2$ $2p^4 3p^2$ ($nl \rightarrow \infty$) (group E). These limits were not indicated in Fig. 1 as the intensity already drops at the first limits. In general, the Auger processes involving excited electrons should be rather rare as the competing optical decays are often allowed and have a larger probability. Only when the decay is optically forbidden, an intense Auger line will result. The fact that mainly the few optically forbidden transitions will lead to Auger intensity may be responsible for the distinct structure of the spectrum which remains observable in spite of an increasing density of possible transitions toward the series limits.[14]

In this work, we are mainly interested in transition energies for the Auger decays of initial states $L_{23}M^i$, $L_{23}^2 M^i$, and $L_{23}^3 M^i$ with mostly large outer-shell ionization. A method to obtain semiempirical energy estimates for some of these cases has been presented recently.[6] This method works as shown in the following example: the two $3p$-electrons in $1s^2 2s^2 2p^5 3p^2$ of P^{4+} with nine electrons in the core roughly feel the field of the screened nucleus of $Z_S = 15-9=6$. The same screened charge is experienced by two $3p$-electrons in $1s^2 2s^2 2p^6 3p^2$ of S^{4+}. Hence, we expect for the terms resulting from $3p^2$ (i.e., ^1S, ^1D, ^3P) in both cases a similar splitting, and a similar energy offset from the mutual "ground states" (i.e., ground states with respect to the outer-shell configuration) $1s^2 2s^2 2p^5 3s^2$ and $1s^2 2s^2 2p^6 3s^2$. This offers the opportunity to derive semiempirical term energies in calculating average energies of these ground states with a Hartree-Fock program,[10] and adding the experimental energy offset and term splitting meas-

ured for the analogous configuration in S^{4+}, which can be taken from tables.[14]

For two reasons, this method is not as powerful as it seems. First, not the term splittings are difficult to calculate, but the absolute values of the average energies. Second, the neglect of the interaction of an unfilled $2p$ shell with the $3p$ electrons may cause a large perturbation of the terms. A comparison of semiempirical and calculated data is shown in Table I for terms of P^{4+} to P^{6+}. The two values are very close for P^{4+} with only one $2p$ vacancy. However, for high inner-shell ionization, as, e.g., P^{6+} with three $2p$ holes, the semiempirical data exceed our calculated relative energies by almost 60%. The typical error of Hartree-Fock calculations is much lower than this derivation and shows the opposite tendency, i.e., the calculated relative energies are always an upper bound. From this we conclude that the semiempirical method produces poor results in the case of a high degree of inner-shell ionization. It is also seen in Table I that the coupling of the incomplete $2p$-shell with the nonclosed outer shell does not only shift term energies but leads to an additional splitting with a multitude of terms spread over several eV. This splitting also becomes more important for states with large inner-shell ionization. In addition, semiempirical energies are only available for a few optically accessible states.

Hartree-Fock calculations for states with inner-shell vacancies are very critical with respect to convergence when states are considered for which a rotation of the orbitals may lead to a configuration with lower energy.[15] Such a rotation may turn a

TABLE I. Comparison of semiempirical and calculated energies for terms of P^{4+} to P^{6+}. Calculated term energies have been averaged statistically to allow for comparison with experimental data.

Calculated			Semiempirical[a]		
	Relative energies (eV)				Equivalent
Term	Term	Average	Average	Term	ion
$2p^5 3s^2\,{}^2P$[b]	0.0	0.0	0.0	$2p^6 3s^2\,{}^1S$	S^{4+}
$2p^5 3s\,3p\,{}^3P({}^4S)$	6.1	8.3	10.4	$2p^6 3s\,3p\,{}^3P$	
^4D	7.6				
^4P	8.6				
^2D	9.0				
^2P	9.3				
^2S	11.2				
$2p^5 3s\,3p\,{}^1P$[c]	15.2	15.8	15.4	$2p^6 3s\,3p\,{}^1P$	
	18.1				
$2p^5 3p^2\,{}^3P$[c]	19.7	21.2	24.5	$2p^6 3p^2\,{}^3P$	
	24.9				
$2p^4 3s^2$[b,c]	−3.2	0.0	0.0	$2p^6 3s^2$	Cl^{5+}
	12.7				
$2p^4 3s\,3p$		10.2	13.8	$2p^6 3s\,3p$	
$2p^4 3p^2$		23.6	29.3	$2p^6 3s\,3p$	
$2p^3 3s^2\,{}^4S$[b]	−9.8	0.0	0.0	$2p^6 3s^2$	Ar^{6+}
^2D	0.0				
^2P	6.6				
$2p^3 3s\,3p$		10.4	16.0	$2p^6 3s\,3p$	
$2p^3 3p^2$		24.1	33.7	$2p^6 3p^2$	

[a]Term splittings from Ref. 15, average energies calculated.
[b]Average energy normalized to be 0.0 eV.
[c]Not all possible final terms are given, but the energies of the lowest and highest terms are indicated.

term $2p^{-1}3p^{-1}\,{}^1S$ into $3p^{-2}\,{}^1S$ with considerably lower energy. These effects can be avoided in performing the HF calculations for those terms that are real ground states considering not only the configuration, but also the angular coupling. The Slater integrals from these calculations may be used to derive the other terms that are not true ground states. The best method would be to calculate first a statistical average of all term energies that are ground states in the above sense,[15] but it has been found that the former method is sufficient for the present work. The discrepancies of the two methods are beyond our limit of observation. We expect that the term energies calculated in this way are correct to within 1 eV.

In order to test the importance of the spin-orbit interaction, the spin-orbit matrix together with the electrostatic contributions has been diagonalized for one case. The results (lower row in Fig. 2) show that the spin-orbit splitting is comparatively small. It is largest for the terms ${}^3P({}^2P)$ with 0.8 eV, ${}^3P({}^4D)$ with 0.6 eV, and ${}^3P({}^2D)$ with 0.5 eV. The splitting is just at the limit of observation in our spectra and will not be calculated for the other configurations. In Fig. 2 we have indicated all allowed Auger transitions with full lines and forbidden transitions with broken lines. This shows that often more than 50% of the transitions are forbidden in pure LS coupling. We expect, however, especially with an increasing number of inner-shell vacancies, an influence of spin-orbit mixing which pulls intensity also toward transitions forbidden in LS coupling. This may actually be an explanation for the general shape of the Auger spectra. They are simple on the low-energy part—nearly line spectra—where spin-orbit interaction is low as few inner-shell holes are present. With increasing energy we approach regions where lines from states with many inner-shell holes prevail. They are numerous due to spin-orbit mixing and lead to a quasicontinuous structure.

Figure 3 shows the low-energy portion of the Auger spectrum together with calculated Auger-transition energies. Transitions forbidden in LS coupling are indicated by broken lines. The assignments are given in Table II. Considering the fact that in Ref. 6 the splitting of terms introduced by the $2p$ vacancy is neglected, we agree mainly with the assignments indicated there (see lines, 2, 4, 7, 10, and 11). For line 2 we would also expect a certain contribution from $L_{23}^3M_{23}^3-L_{23}^2M_1^2M_{23}^3$ transitions. This contribution should be important in case that line 1 is due to a $L_{23}^3M_{23}^3-L_{23}^2M_1^2M_{23}^2$ decay as discussed later. Considering line 4, we assume that it consists of a blend of lines of the type $2p^5\,3s\,3p^3P({}^{2S+1}L)-2p^6\,{}^1S$. The same fact is expressed in Ref. 6 by neglecting the splitting into terms in the notation $2p^5\,3s\,3p^3P-2p^6\,{}^1S$. As there is an isolated transition $2p^5\,3s\,3p^3P$ $({}^2S_{1/2})-2p^6\,{}^1S$ near line 6, we can give a clear assignment here. Line 7 can be assigned to two transitions $2p^5\,3s\,3p\,{}^1P({}^2D_{1/2,5/2})-2p^6({}^1S)$. In Ref. 6 the initial terms are not fully specified; only the intermediate ${}^1P$ coupling is given. In the case of line 9 we give an assignment deviating from Ref. 6. Our calculations indicate that this still belongs to the group of $2p^5 3s\,3p-2p^6$ decays. Our assignment of line 10 is again more specific than Ref. 6 and refers to the transition $2p^5(3p^{21}D)$ $({}^2F)-2p^6\,{}^1S$—allowed in LS coupling.

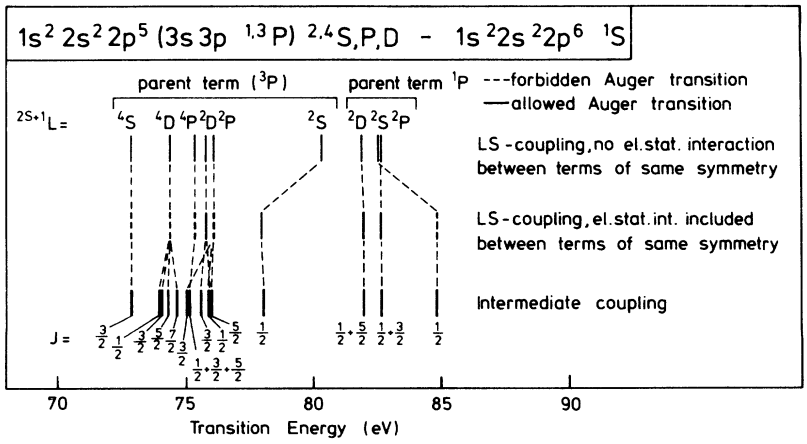

FIG. 2. Calculated transition energies for Auger transitions of terms $1s^22s^22p^5(3s\,3p^{1,3}P)^{2,4}S,P,D-1s^22s^22p^6\,{}^1S$. Starting with LS-coupling data for single terms, first the electrostatic interaction between states with the same L and S and finally also the spin-orbit splitting is included.

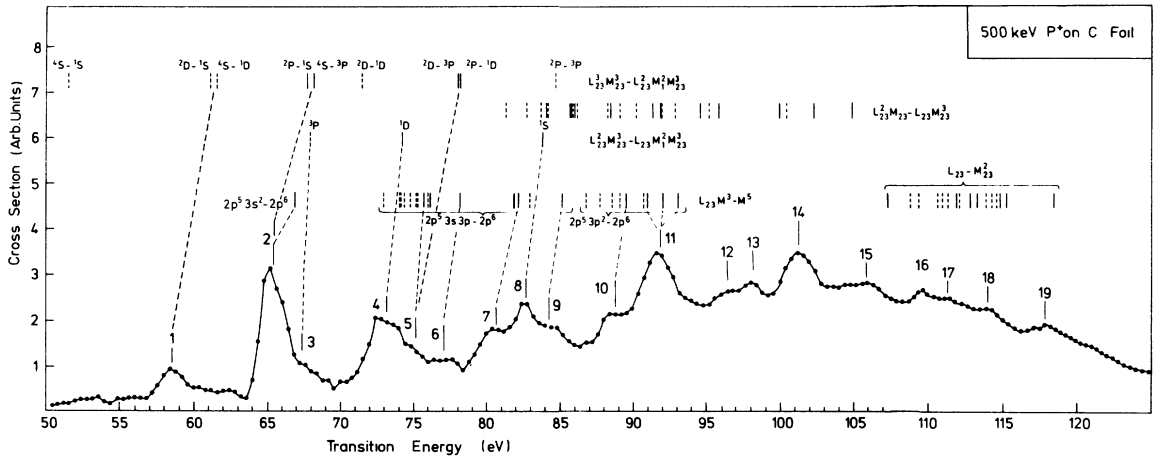

FIG. 3. *P*-Auger spectrum following 500-keV P^+ impact on C_{foil}. Energies are calculated in *LS* coupling. Allowed lines (full bar) and forbidden lines (broken bar) are distinguished; * marks most important groups.

Line 11 is broad and should be due to three transitions allowed in *LS* coupling: $2p^5 3p^2\,{}^3P,{}^1D,{}^1S({}^2P)-2p^6\,{}^1S$. So, our calculations allow for a slightly more precise determination of the terms in the decays considered.

In Fig. 3 no allowed transition of the type $L_{23}M^i-L_{23}^{i-1}M^{i+2}(i=1,2)$ could be proposed for which is not very intense but is present in all our spectra. Our first suggestion is that it belongs to transitions forbidden in *LS* coupling of the type $2p^3 3s^2-2p^4$ with the initial terms $({}^2D)$ and $({}^4S)$ and the final terms $({}^1S)$ and $({}^1D)$, respectively. This assignment, however, is still very questionable as we should then expect to observe strong lines at the calculated positions for the allowed transitions of the same group. This is not the case unless we shift the whole group down in energy by 3 eV until the transitions $({}^2P)-({}^1S)$ and $({}^4S)-({}^3P)$ match with line 2. This shift may be realistic although the excitation of a triply ionized inner shell seems very unlikely.

Other candidates for line 1 are Coster-Kronig transitions involving highly excited electrons. Usually, Coster-Kronig transitions are found at very low energies compared with the normal Auger transitions of the same shell. If at least one of the electrons participating in the Coster-Kronig decay is already highly excited in the initial state, it has to overcome only a very weak binding. Hence, the transition energy of these decays may be considerably higher than the energies of normal Coster-Kronig transitions. Table III shows calculated energies for these two types of transitions. The energy of the transition $1s^2 2s\,2p^6 3s^2 3p^3 3d - 1s^2 2s^2 2p^5 3s^2 3p^3$ is only 2 eV lower than line 1; so it may be a candidate. Otherwise we know that Coster-Kronig transitions are always much faster than the corresponding Auger transitions. This leads to rather large linewidths. In our case, the observed linewidths are influenced by the kinematic broadening, and statements on the natural widths are not very accurate. It seems, however, that line 1 has only a small width ($\lesssim 10$ meV). The information available from this line does not yet suffice to draw a decisive conclusion.

The main intensity (e.g., for 500-keV impact energy) is found in the intermediate region between 90 and 110 eV (see Fig. 1), where we expect also the normal $2p$-Auger decays. In analogy with other spectra[3,9,16] the strongest transitions will be of the type $L_{2,3}-M_{23}^2$. The other groups $L_{23}-M_1M_{23}$ and $L_{2,3}-M_1^2$ will be of lower intensity. For the $L_{2,3}-M_{23}^2$ transitions the complete term splitting has been calculated (Table III) and the results are shown in Fig. 3. It is seen that the majority of our calculated transition energies fits into a broad structure in the spectrum (lines 16–18). Eventually also lines 15 and 19 belong to this group.

According to Fig. 1 the high-energy portion of the spectrum is mainly due to two types of transitions: first, Auger decays of states with two vacancies in the $2p$ shell and few vacancies in the outer shell; second, decays of states with one or two inner-shell vacancies and an outer-shell electron being excited to higher orbitals. The latter states may be produced by excitation of the inner-shell electron or by capture of an electron following the inner-shell ionization. These transitions of types B_α and B_β should lead to intensity near 117

TABLE II. Proposed assignments of lines 1 – 11 based on calculated energies.

Line	Transition	Degree of 2p ionization	Ref. 6
1	$2p^3 3s^2\,^2D - 2p^4\,^1S$	3 +	
	$+2p^3 3s^2\,^4S - 2p^4\,^1D$	3 +	
	and/or terms of		
	$2s\,2p^6 3s^2 3p^3 3d - 2s^2 2p^5 3s^2 3p^3$	0	
2	$2p^5 3s^2\,^2P - 2p^6\,^1S$	1 +	same
	$+2p^3 3s^2\,^2P - 2p^4\,^1S$	3 +	
	$+2p^3 3s^2\,^4S - 2p^4\,^3P$	3 +	
4	Terms of $2p^5 3s\,3p^3P(^{2S+1}L) - 2p^6\,^1S$		
	$+2p^4 3s^2\,^1D - 2p^5\,^2P$	2 +	$2p^5 3s\,3p^3P - 2p^6\,^1S$
5	$2p^5 3s\,3p^3P(^2D_{1/2}) - 2p^6\,^1S$ and/or similar terms	1 +	
	$+2p^3 3s^2\,^2D - 2p^4(^3D)$		
	$+2p^3 3s^2\,^2P - 2p^4(^1D)$		
6	$2p^5 3s\,3p^3P(^2S_{1/2}) - 2p^6\,^1S$	1 +	
7	$2p^5 3s\,3p^1P(^2D_{1/2,5/2}) - 2p^6\,^1S$	1 +	$2p^5 3s\,3p^1P - 2p^6\,^1S$
8	$2p^4 3s^3\,^1S - 2p^5\,^2P$	2 +	
9	$2p^5 3s\,3p^1P(^2S) - 2p^6\,^1S$	1 +	$2p^5 3p^2\,^2P - 2p^6\,^1S$
10	$2p^5 3p^2\,^1D\,(^2F) - 2p^6\,^1S$	1 +	$2p^5 3p^2\,^1D - 2p^6\,^1S$
11	$2p^5 3p^2\,^3P,^1D,^1S\,(^2P) - 2p^6\,^1S$	1 +	$2p^5 3p^2\,^1S - 2p^6\,^1S$

and 127 eV, respectively.

For completeness, the possibility of 2s-Auger decays should be mentioned. The transition energies are in most cases considerably larger than the spectrum displayed in Fig. 2. In our experiment we did not find any discrete structure near the calculated energies. We conclude that also the lowest transitions of this type between 90 and 130 eV will not contribute considerably to the observed structure and can be neglected.

TABLE III. Calculated transition energies for Coster-Kronig decays involving excited electrons and outer-shell vacancies.

Transition	Calculated energy (eV)
$1s^2 2s\,2p^6 3s^2 3p^3 3d - 1s^2 2s^2 2p^5 3s^2 3p^3$	56.74
$1s^2 2s\,2p^6 3s^2 3p^3 4s - 1s^2 2s^2 2p^5 3s^2 3p^3$	55.28
$1s^2 2s\,2p^6 3s^2 3p^3 4p - 1s^2 2s^2 2p^5 3s^2 3p^3$	56.18
$1s^2 2s\,2p^6 3s^2 3p^3 - 1s^2 2s^2 2p^5 3s^2 3p^2$	35.25
$1s^2 2s\,2p^6 3s^2 3p^3 - 1s^2 2s^2 2p^5 3s\,3p^3$	24.45
$1s^2 2s\,2p^6 3s^2 3p^2 - 1s^2 2s^2 sp^5 3s^2 3p$	25.82
$1s^2 2s\,2p^6 3s^2 3p^2 - 1s^2 2s^2 2p^5 3s\,3p^2$	15.54
$1s^2 2s\,2p^6 3s^2 3p - 1s^2 2s^2 2p^5 3s^2$	13.07
$1s^2 2s\,2p^6 3s^2 3p - 1s^2 2s^2 2p^5 3s\,3p$	3.44
$1s^2 2s\,2p^6 3s^2 - 1s^2 2s^2 2p^5 3s$	energetically
$1s^2 2s\,2p^6 3s - 1s^2 2s^2 2p^5$	forbidden

IV. INTENSITY CONSIDERATIONS

As mentioned in the beginning, attention has been drawn to the present collision system from observations of very high Auger yields for the P^+ projectile[1] following foil excitation. In contrast to excitation by gases at low pressure, the projectile traversing a foil suffers many collisions mostly at a very rapid succession. This may lead to multiply excited states. The Auger electrons measured here originate to a large part from outside the foil.[4] Thus, they yield information on the state of the projectile reached after many succeeding collisions involving many excitation and deexcitation processes.

In the above-mentioned study[1] it has been observed that the Auger yield is nearly constant from 100- to 500-keV impact energy. Based on those measurements of absolute Auger yields, we could normalize our spectra and present relative cross sections (Fig. 4). In comparing these spectra, we have to keep in mind that the structures are broadened by kinematical effects, especially for lower impact energies.

Before discussing the impact-energy dependence of our spectra, we compare the 500-keV data with an earlier experiment[6] using 50-keV impact energy and an Ar gas target. The two spectra are very similar besides of a little more intensity at high electron energies in our case. The gas-excited spectrum has been explained[6] to be due mainly to cascading transitions $L^2-LM^2-M^4$. The corresponding transition energies lie in the ranges 100–140 eV (L^2-LM^2) and 60–100 eV (LM^2-M^4). The intensities of the two spectral regions were found to be equal in intensity, thus supporting the cascade hypothesis. In the low-energy portion (60–100 eV) we also expect a contribution from single inner-shell ionization, which has been found to be comparatively small for excitation by Ar gas.[5] For our foil-excited spectra, no prediction about this contribution can be made because of the complex excitation process.

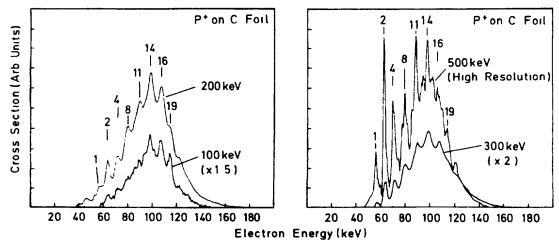

FIG. 4. Phosphorus-projectile Auger spectra at different impact energies excited by a 10-μg/cm^2 carbon foil. The observation angle was 9° with respect to the incident beam.

The most important feature of the foil-excited spectra is the appearance of a more intense high-energy portion growing with decreasing impact energy. This behavior leads to a shift of the centroid energy toward higher energies. There are mainly two possibilities to explain the new feature: (i) $L^2M^i-LM^{i+2}$ transitions increasing for low impact energies (according to the electron-promotion model[17] accompanied by single ionization dominating at high impact energy and decreasing for low impact energies and (ii) capture of electrons into excited orbitals from the surface of the foil.

An increase of L^2-LM^2 transitions (100–140 eV) for low impact energies should also lead to an increase of LM^2-M^4 decays (60–100 eV) due to cascading. This increase is, however, not observed. A possible explanation for this may be the low-energy spectrum is due only to one part to LM^2-M^4 transitions fed by the cascading process $L^2-LM^2-M^4$ and to the other part to direct single inner-shell ionization. The cascading ratio of approximately 1:1 found for Ar excitation may be reduced by competing optical decays. In this way, the low-energy portion may be dominated by decays following direct single inner-shell ionization. Hence, an increase of the transitions L^2-LM^2 will not influence much the low-energy portion. This hypothesis could be tested by measurements of optical decays.

Another explanation for the observed change of our spectra as a function of the impact energy can be given in considering the peculiarities of the foil-excitation process. When the projectile leaves the foil, it can easily pick up electrons from the surface. States involving inner-shell vacancies and additional electrons in the outer orbitals are formed, e.g., $2p^5 3s^k 3p^i nl$. The transition energies of these states are found on the high-energy part of the spectrum up to the limits indicated in Fig. 1. Also, this process should lead to many optical transitions, which should be measured to support this assumption. As the probability for this charge transfer from the foil to the projectile will increase with decreasing impact energy, the energy dependence of the spectra can be understood. We expect that this process is very important for our foil-excited spectra, as a similarly strong high-energy part is missing in the spectra excited by Ar gas.[6]

In the following the intensity variations of the individual lines are discussed. For the first two

lines we observe an increase of intensity with increasing projectile energy. As the identification of peak 2 to be due to the transition $2p^5 2s^2\,{}^2P - 2p^6\,{}^1S$ is rather sure, we can draw the conclusion that in fast collisions the production of initial states with one inner-shell vacancy and many outer-shell vacancies prevails. Lines 5, 6, 7, and 9 are other candidates for similar transitions. Collisions with a solid target are very effective in disrupting the outer shells. But we do not expect that a very high degree of ionization occurs in the inner shells at high projectile energies.

A similar intensity variation is observed for line 1 (see Fig. 4) which may be due to decays of initial states with a high degree of inner-shell ionization in addition to a nearly depleted outer shell, i.e., $2p^3 3s^2 - 2p^4$, or to Coster-Kronig transitions with an active spectator electron. The similarity of the intensity variations of lines 1 and 2 indicates that line 1 might also be due to an initial state with a single inner- and many outer-shell vacancies. The proposed Coster-Kronig decay may originate from such an initial state after capture of electrons into the outer shells. However, we would assume a much lower intensity for such a process.

For lines 4, 8, 11, 14, and 16 we observe a totally different tendency. In the first two cases, lines 4 and 8, no explicit energy dependence can be observed. For the unresolved lines 7 and 8 we observe a maximum of the peak at 200–300 keV impact energy. However, the two high-energy spectra indicate a very different behavior of the now distinct lines composing this peak. Line 8 is nearly constant, whereas line 7 decreases strongly from 300 to 500 keV. The opposite impact-energy dependence of these two lines is in close agreement to our identification: line 7 is due to the decay of a single inner-shell vacancy, line 8 to the decay of a double inner-shell vacancy. Also the analogy of line 4 and line 8 is consistent with the assignment of line 4 to be due to an initial state with two $2p$ vacancies. In the case of lines 11, 14, and 16 we find a clear maximum of the intensity near 300, 200, and 200 keV, respectively. This variation indicates that these lines should not be due to decays of single inner-shell vacancies. For line 11 this means that our assignment as a transition of the type $2p^5 3p^2 - 2p^6$ is not representative for the main intensity of this peak. In the case of peak 16 we think that at high impact energies the observed structure is really due to $L_{23} - M_{23}^2$ decays. With decreasing projectile energy this structure is shadowed by decays of double $2p$ vacancies, thus also changing the shape of the peak. For lines 3 and 10 no intensity arguments can be given because they are found on the slopes of very strong neighboring lines.

V. CONCLUSIONS

Our analysis of the phosphorus Auger spectrum has shown that a spectroscopic analysis is possible to some extent in the low-energy region of the spectrum where discrete structures can be well resolved. The overall shape of the spectrum at different excitation energies can be understood assuming increased charge exchange and/or double L_{23} vacancy production at lower impact energies. In the very low-energy portion of the spectrum a faint structure seems to indicate either a Coster-Kronig decay of a configuration with single $2s$ ionization and high excitation of the electronic shells or triple ionization of the $2p$ shell. This structure deserves further investigations. Theoretical data on initial populations and transition rates for lines in this region could be of great help in future examinations. The supposed charge-exchange processes at low impact energy could also lead to intensity in the optical region. Hence, optical measurements would be of great importance for the further study of the excitation of phosphorus ions by foils.

We thank Professor Dr. W. Mehlhorn for a reading of the manuscript and many helpful comments and suggestions.

---

*Present address: D-8000 Munchen 50, Georg-Reismuller-Strasse 39, West Germany.

[1]D. Schneider, N. Stolterfoht, D. Ridder, H. C. Werner, R. J. Fortner, and D. L. Matthews, in Proceedings of the Fifth Conference on Scientific and Industrial Applications of Smaller Accelerators, Report No. 76 CH 117-9 NTS (North Texas State University, Denton, Texas, 1978), p. 1136 (unpublished).

[2]R. A. McCorkle, Phys. Rev. Lett. 29, 983 (1972).

[3]W. Mehlhorn and W. N. Asaad, Z. Phys. 191, 231 (1966); W. Mehlhorn and D. Stahlherm, *ibid.* 217, 294 (1968).

[4]D. Schneider, R. Bruch, W. H. E. Schwarz, T. C. Chang, and C. F. Moore, Phys. Rev. A 15, 926 (1977); R. Bruch, D. Schneider, W. H. E. Schwarz, M. Meinhart, B. M. Johnson, and K. Taulbjerg, *ibid.* 19, 587 (1979).

[5]B. Fastrup, G. Herman, and K. J. Smith Phys. Rev. A 3, 1591 (1971).

[6]P. Dahl, M. Rødbro, G. Herman, B. Fastrup, and M. E. Rudd, J. Phys. B 9, 1581 (1976).

[7]L. Viel, C. Benazeth, and N. Benazeth, Surf. Sci. 54, 635 (1976).

[8]N. Stolterfoht, D. Schneider, D. Burch, B. Aagaard, E. Bøving, and B. Fastrup, Phys. Rev. A 12, 1313 (1975).

[9]M. O. Krause, T. A. Carlson, and W. E. Moddemann, J. Phys. (Paris) 32, C4-139 (1971).

[10]C. Froese-Fischer, Comput. Phys. Commun. 4, 107 (1972).

[11]A. Hibbert, Comput. Phys. Commun. 1, 359 (1969).

[12]W.-D. Klotz, Comput. Phys. Commun. 9, 102 (1975).

[13]N. Stolterfoht, D. Schneider, D. Burch, D. Aagaard, E. Boving, and B. Fastrup, Phys. Rev. A 12, 1313 (1975).

[14]C. E. Moore, *Atomic Energy Levels,* Vol. I, Circular No. 467 (National Bureau of Standards, Washington, D. C., 1949).

[15]C. Froese-Fischer and D. Ridder, J. Phys. B 11, 2267 (1978).

[16]D. Ridder, N. Stolterfoht, and G. Wustefeld, in *Proceedings of the Tenth International Conference on the Physics of Electronic and Atomic Collisions, Paris, 1977,* edited by G. Watel (North-Holland, Amsterdam, 1978), p. 212.

[17]V. V. Afrasimov, Yu. S. Gordeev, A. N. Zinoviev, D. H. Rasulov, and A. P. Shergin (unpublished).